Inorg. Chem. **2005**, *44*, 1302–1308

Structural Characterization of an Enantiopure Hydroxo-Bridged Binuclear Iron(III) Complex with Empty One-Dimensional Helical Channels

Md. Akhtarul Alam,[†] Munirathinum Nethaji,*[,‡] and Manabendra Ray*[,†]

Department of Chemistry, Indian Institute of Technology Guwahati, Guwahati 781039, India, and Department of Inorganic and Physical Chemistry, Indian Institute of Science, Bangalore 560012, India

Received June 30, 2004

A H-bond capable chiral tetradentate ligand, Fe^{3+}, and acetate ion assembles into a hydroxo-bridged binuclear complex with the formula $[Fe^{III}_2(\mu\text{-OH})(\mu\text{-OAc})(S\text{-L})_2]\cdot 4H_2O$ (**1**) where H_2S-L = *S*-2-(2-hydroxy-benzylamino)-3-(1*H*-imidazol-4-yl)-propionic acid. The crystal of **1** contains right-handed one-dimensional (1D) helical channels with 7.3–9.8 Å diameter. A similar reaction with a ligand having opposite chirality forms the complex with left-handed helical channels (**1a**). Heating the crystals of **1** at 95 °C under reduced pressure selectively removes three waters from the channel forming an enantiopure porous crystal with empty channels (solvent accessible voids 18% v/v). Intermolecular hydrogen bonding between the imidazole N–H and phenolate oxygen in **1**–**2** forms a C_6 symmetric helix with bridging hydroxo groups pointing inside the channels. All the H-bond capable atoms in the ligand along with one water molecule form an extended H-bonded network throughout the crystal. Exposing the empty channels of **2** to iodine vapor indicates partial filling of the channels with iodine. Crystal data for $\mathbf{1}\cdot 4H_2O$ include the following: hexagonal, $P6_1$, $a = b = 13.164(3)$ Å, $c = 36.305$ (11) Å, $\alpha = \beta = 90°$, $\gamma = 120°$, $Z = 6$, R1 = 0.0387, wR2 = 0.0842. Crystal data for $\mathbf{1a}\cdot 2H_2O$ include the following: hexagonal, $P6_5$, $a = b = 13.151(4)$ Å, $c = 36.558(2)$ Å, $\alpha = \beta = 90°$, $\gamma = 120°$, $Z = 6$, R1 = 0.0416, wR2 = 0.1190. Crystal data for $\mathbf{2}\cdot H_2O$ include the following: hexagonal, $P6_1$, $a = b = 13.160(7)$ Å, $c = 36.559$ (4) Å, $\alpha = \beta = 90°$, $\gamma = 120°$, $Z = 6$, R1 = 0.0574, wR2 = 0.1423.

Introduction

Porous solids with channels of different pore diameter have been synthesized because of their use or anticipated use as template to synthesize nanofibers, one-dimensional array of molecules, sensors, ion exchangers, and catalysts.[1] Enantiopure one-dimensional (1D) channels have advantages over achiral solids for use in chiral separation, transformation, and nonlinear optical material.[2,3] Few materials with 1D chiral channels have been synthesized using a chiral[2,4] or achiral[5] ligand metal complex. Out of these, three have been synthesized in the enantiomerically pure form,[2b,4] and of them two[4] contain 1D helical channels. Common problems associated in the synthesis of such material are (a) formation of channel with ions blocking the channel[6] and (b) collapse of the lattice[4b] during thermal removal of solvents or neutral

* To whom correspondence should be addressed. E-mail: manabray@iitg.ernet.in.
† Indian Institute of Technology Guwahati.
‡ Indian Institute of Science.

(1) (a) Davis, M. E. *Nature* **2002**, *417*, 813. (b) Yaghi, O. M.; Li, H.; Davis, C.; Richardson, D.; Groy, T. L. *Acc. Chem. Res.* **1998**, *31*, 474. (c) Ikegame, M.; Tajima, K.; Aida, T. *Angew. Chem., Int. Ed.* **2003**, *42*, 2154. (d) Kitaura, R.; Kitagawa, S.; Kubota, Y.; Kobayashi, T. C.; Kindo, K.; Mita, Y.; Matsuo, A.; Kobayashi, M.; Chang, H. C.; Ozawa, T. C.; Suzuki, M.; Sakata, M.; Takata, M. *Science* **2002**, *298*, 2358. (e) Kitagawa, S.; Kitaura, R.; Noro, S. *Angew. Chem., Int. Ed.* **2004**, *43*, 2334.
(2) (a) Kesanli, B.; Lin, W. *Coord. Chem. Rev.* **2003**, *246*, 305. (b) Seo, J. S.; Whang, D.; Lee, H.; Jun, S. I.; Oh, J.; Jeon, Y. J.; Kim, K. *Nature* **2000**, *404*, 982.
(3) Langley, P. J.; Hulliger, J. *Chem. Soc. Rev.* **1999**, *28*, 279.
(4) (a) Noord, A. D. C.-V.; Kampf, J. W.; Pecoraro, V. L. *Angew. Chem., Int. Ed.* **2002**, *41*, 4668. (b) Wu, C.-D.; Lu, C.-Z.; Lu, S.-F.; Zhuang, H.-H.; Huang, J.-S. *Dalton Trans.* **2003**, 3192..
(5) Kniep, R.; Will, H. G.; Boy, I.; Röhr, C. *Angew. Chem., Int. Ed. Engl.* **1997**, *36*, 1013.
(6) Smithson, R. J.; Kilner, C. A.; Brough, A. R.; Halcrow, M. A. *Polyhedron* **2003**, *22*, 725.

10.1021/ic049145n CCC: $30.25
Published on Web 01/27/2005

molecules blocking the channel. None of the previous 1D helical channels containing crystals has been characterized in the empty form.

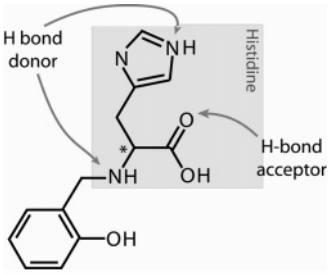

H_2 *S*-L

In our earlier attempts to use metal coordination and H-bonds in the formation of molecular assembly, we had observed that amino acid derived tetradentate ligands, H_2*S*-L, have a tendency to form a H-bonded network due to the presence of a complementary H-bond donor and acceptor (imidazole, carboxylate) in the same ligand.[7] The use of natural amino acids synthesizing the ligand makes the induction of chirality in the complex easier and cheaper. The presence of a phenolate donor is expected to give a strong charge-transfer (CT) transition to metal complexes with iron(III). The presence of a strong CT transition is one of the requirements for second-order nonlinear optical materials. In this paper, we report the synthesis and characterization of a hydroxo-bridged binuclear iron(III) complex which forms crystals with parallel one-dimensional helical channels (7−9 Å diameter). H-bonded water from the channel could be thermally removed to form empty channels without destroying the lattice. Further, the accessibility of the empty channels toward small molecules was explored with iodine.

Experimental Section

Materials and Methods. Reagents were purchased from commercial sources and, unless otherwise stated, were used as received. MeOH was distilled over magnesium methoxide following the standard procedure. L-Histidine and imidazole were brought from Sisco Research Laboratories Pvt. Ltd. (SRL), India, and used as received. Salicylaldehyde was purchased from Sigma-Aldrich Co. and used without further purification. The ligand H_2*S*-L (*S*-2-(2-hydroxy-benzylamino)-3-(1*H*-imidazol-4-yl)-propionic acid), $[\alpha]^{25}_D = -75$ (*c* 0.772 in MeOH in the presence of 2 equiv of LiOH), was synthesized and characterized using elemental analysis, ESI-MS, ^{1}H NMR, and IR as reported earlier.[7]

The IR spectra were recorded on a Nicolet Impact 410 FT-IR spectrophotometer with KBr disks in the range 4000−400 cm^{-1} and electronic spectra on a Shimadju U-2001 spectrophotometer. The thermogravimetric analyses (TGA) of the compounds were performed by using an SDTA 851e TGA thermal analyzer (Mettler Toledo) with a heating rate of 5 °C per min in a N_2 atmosphere using a sample size of 5−10 mg per run. Solid-state magnetic susceptibility of the complexes at room temperature was recorded using Sherwood Scientific balance MSB-1. Solution electrical conductivity measurements were made with a Systronics Conductivity meter 306 by using 0.01 N KCl solution as calibrant. Elemental analyses were done using a Carlo Erba 1108 and also by using a Perkin-Elmer series II 2400 instrument. ESI-MS for ligands were done using a Micromass Quattro II mass spectrometer. Optical rotations were measured using a Perkin-Elmer 343 polarimeter.

***R*-2-(2-Hydroxy-benzylamino)-3-(1*H*-imidazol-4-yl)-propionic Acid (H_2*R*-L).** This was synthesized starting with D-histidine mono hydrochloride instead of L-histidine monohydrochloride following the procedure reported for H_2*S*-L.[7] Yield: 70%. IR (KBr, cm^{-1}) ν(COO)$_{asym}$ 1604; ν (COO)$_{sym}$ 1408. *m*/*z* (ESI-MS, [M − H]$^-$) 260. The ^{1}H NMR spectra for the ligand were recorded for the lithium salt of the ligand, prepared by adding 2 equiv of LiOH·H_2O in MeOH and subsequently evaporating MeOH. ^{1}H NMR of Li_2L (CD_3OD, 300 MHz, ppm): 2.75 (dd, 1H, −C**H**H-imidazole), 3.07 (dd, 1H, −CH**H**-imidazole) 3.31 (m, 1H, −C**H**-CH_2), 3.35 (d, 1H, −C**H**H -phenolate), 3.80 (d, 1H, CH**H** -phenolate), 6.37(t, 1H, *p*-phenolate), 6.63 (d, 1H, *o*-phenolate), 6.86 (m, 2H, *m*-phenolate and imidazole), 6.95 (t, 1H, *m*-phenolate), 7.57 (s, 1H, imidazole). Optical rotation: $[\alpha]^{25}_D = +74$ (*c* 0.772 in MeOH in the presence of 2 equiv of LiOH).

[Fe_2(μ-OH)(μ-OAc)(*S*-L)$_2$]·4H_2O (1). Complex **1** was synthesized by adding a methanolic (10 mL) solution of $Fe(NO_3)_3$·9H_2O (0.592 g, 1.46 mmol) to a stirred methanolic (20 mL) solution of H_2*S*-L (0.383 g, 1.46 mmol) and NaOH (0.117 g, 2.93 mmol), followed by addition of NaOAc·3H_2O (0.598 g, 4.39 mmol) in 5 mL of MeOH. The final color of the solution is reddish purple. The solution stirred for 15 min. The volume of the solution was reduced to ∼10 mL, and diethyl ether was added. Cooling the solution in the refrigerator for 3 days yielded dark colored diamond shaped crystals of composition **1**·4H_2O. The crystals were washed with ether and dried in a vacuum desiccator (yield, 65%). All further studies including X-ray structural studies were done on these crystals. However, recrystallization from MeOH occurs in the presence of dilute acid ($HClO_4$ or CH_3COOH to prevent deprotonation of bridging hydroxyl group). Anal. Calcd for $Fe_2C_{28}H_{37}N_6O_{13}$: C, 43.20; H, 4.92; N, 10.79. Found: C, 43.39; H, 4.56; N, 10.81. IR (KBr, cm^{-1}) ν(OH) 3405 (broad); ν(ligand carboxylate)$_{asym}$ 1644; ν (ligand carboxylate)$_{sym}$ 1384; for bridge ν (OAc)$_{asym}$ 1542; ν (OAc)$_{sym}$ 1457; ν (NH) 3110; ν (phenolic, CO) 1270. Λ_M: (MeOH), 12 S cm^{-2} mol^{-1}. UV−vis (0.5 mM in MeOH): λ_{max} [nm] (ϵ [M^{-1} cm^{-1}]), 273 (11300), 302 (sh), 481 (2900). μ_{eff} (powder, 298 K) 4.57 μ_B/iron. TGA: weight loss (average of three measurement) between 30 and 100 °C is 5.7% (calculated for 3H_2O loss 6.94%), and loss between 100 and 140 °C is 2.0% (calculated for 1H_2O loss 2.3%).

[Fe_2(μ-OH)(μ-OAc)(*R*-L)$_2$]·2H_2O (1a). This was synthesized following the procedure described for **1** using H_2*R*-L instead of H_2*S*-L. Yield: 60%. Anal. Calcd for $C_{28}H_{34}Fe_2N_6O_{11}$: C, 45.30; H, 4.61; N, 11.32. Found: C, 45.38; H, 5.24; N, 11.37. IR (KBr, cm^{-1}) ν (OH) 3405 (broad); ν (ligand carboxylate)$_{asym}$ 1644; ν (ligand carboxylate)$_{sym}$ 1384; for bridge ν (OAc)$_{asym}$ 1542; ν (OAc)$_{sym}$ 1457; ν (NH) 3110; ν (phenolic,CO) 1270. Λ_M: (MeOH), 20 S cm^{-2} mol^{-1}. UV−vis (0.5 mM in MeOH): λ_{max} [nm] (ϵ [M^{-1} cm^{-1}]), 273 (12 300), 302 (sh), 480 (2800). μ_{eff} (powder, 298 K); 4.38 μ_B/iron. TGA: weight loss between 35 and 95 °C is 2.34% (calculated for H_2O loss 2.42%), and loss between 95 and 140 °C is 1.93% (calculated for 1H_2O loss 2.42%).

[Fe_2(μ-OH)(μ-OAc)(*S*-L)$_2$]·H_2O (2). Crystals of **2** were obtained by drying crystals of **1** at 95 °C under reduced pressure for 2 h. X-ray diffraction studies were done on these crystals sealed in a capillary to avoid moisture. IR and UV−vis of these crystals were

(7) H_2*S*-L = *S*-2-(2-hydroxy-benzylamino)-3-(1*H*-imidazol-4-yl)-propionic acid. A tetradentate ligand synthesized by reducing Schiff base of L-histidine and salicylaldehyde: Alam, M. A.; Nethaji, M.; Ray, M. *Angew. Chem., Int. Ed.* **2003**, *42*, 1940.

identical with that of **1**. Anal. Calcd for $C_{28}H_{32}Fe_2N_6O_{10}$: C, 46.43; H, 4.45; N, 11.60. Found: C, 46.68; H, 4.74; N, 12.08. TGA: weight loss between 30 and 95 °C is negligible, and loss between 95 and 140 °C is 1. 83% (calculated for $1H_2O$ loss 2.42%).

$[Fe_2(\mu\text{-OH})(\mu\text{-OAc})(S\text{-L})_2]\cdot H_2O\cdot 0.6I_2$ (3). Crystals of **1** dried at 95 °C under reduced pressure for 2 h (**2**). A 50 mg portion of **2** in a vial along with another vial containing solid I_2 were kept inside a round-bottom flask (50 mL) containing dry silica gel to minimize moisture content. This setup was evacuated first and then warmed to 40 °C for few minutes. This was done to remove air (moisture) as much as possible, and heating ensured production of enough I_2 vapor to fill the void. The setup was kept this way for 5−7 days to saturate the crystals with iodine. The I_2 content of the crystals was measured spectrophotometrically (described below). Anal. Calcd for $C_{28}H_{32}Fe_2N_6O_{10}\cdot 0.6I_2$: C, 38.36; H, 3.67; N, 9.58; I, 17.37. Found: C, 36.10; H, 3.38; N, 8.08; I, 17.

Estimation of I_2 Adsorbed in the Crystal (3). The iodine doped crystals (**3**) were put into the fresh CCl_4 (∼6 mL measured), and 6 mL of water was added in the mixture. The mixture was shaken. Complex **1** is insoluble in CCl_4. The CCl_4 layer became strongly purple due to the released I_2 while the iron complex being water soluble stayed in the water layer. The CCl_4 layer was separated, and the I_2 concentration was measured spectrophotometrically.

X-ray Crystallography. Single crystals of **1** and **1**a were grown from reaction mixture by slow diffusion of diethyl ether. The crystals of **2** were obtained by drying crystals of **1** at 95 °C under reduced pressure for 2 h. Complex **2** was mounted on a glass fiber to prevent absorption of moisture. The intensity data for **1**, **1a**, and **2** were collected using a Bruker SMART APEX CCD diffractometer, equipped with a fine focus 1.75 kW sealed tube Mo Kα X-ray source, with increasing ω (width of 0.3° per frame) at a scan speed of 3 s/frame. The SMART software was used for data acquisition and the SAINT software for data extraction. Absorption corrections were done using SDABS only as other kinds of absorption did not help.[8] Structures were solved and refined using SHELX97.[9] All non-hydrogen atoms were refined anisotropically. The solvent water molecules were disordered and shared the occupancies, and the hydrogen atoms attached to them could not be located or fixed, so the molecular weight may not match in all the cases. As the water molecules in the channel were disordered, unrealistic intra/intermolecular contacts are seen. The hydrogen atoms were located from the difference Fourier maps and refined, so some of the C−H bond will not be ideal and may vary. Selected crystallographic data are summarized in Table 1.

Table 1. Crystal Data and Structure Refinement for **1**, **1a**, and **2**

	1	**1a**	**2**
empirical formula	$C_{28}H_{37}Fe_2N_6O_{13}$	$C_{28}H_{32}Fe_2N_6O_{11}$	$C_{28}H_{32}Fe_2N_6O_{10}$
fw	777.34	740.30	724.30
temp	293(2)	293(2)	293(2)
radiation	Mo Kα	Mo Kα	Mo Kα
wavelength	0.71073 Å	0.71073 Å	0.71073 Å
cryst syst	hexagonal	hexagonal	hexagonal
space group	$P6_1$	$P6_5$	$P6_1$
$a = b$, Å	13.164(3)	13.151(4)	13.161(7)
c, Å	36.305(11)	36.56(2)	36.56(4)
$\alpha = \beta$, deg	90.00	90.00	90.00
γ, deg	120.00	120.00	120.00
V, Å^3	5449(2)	5476(4)	5484(7)
Z	6	6	6
ρ	1.421	1.347	1.316
μ	0.866	0.854	0.850
$F(000)$	2418	2292	2244
reflns collected	42827	56517	41609
indep reflns	7101	7816	7704
refinement method	*a*	*a*	*a*
GOF	0.995	1.199	1.133
final R indices $[I > 2\sigma(I)]$	R1 = 0.0387	R1 = 0.0416	R1 = 0.0574
	wR2 = 0.0842	wR2 = 0.1190	wR2 = 0.1423
R indices (all data)	R1 = 0.0488	R1 = 0.0461	R1 = 0.0747
	wR2 = 0.0879	wR2 = 0.1235	wR2 = 0.1525

[a] Full-matrix least-squares on F^2.

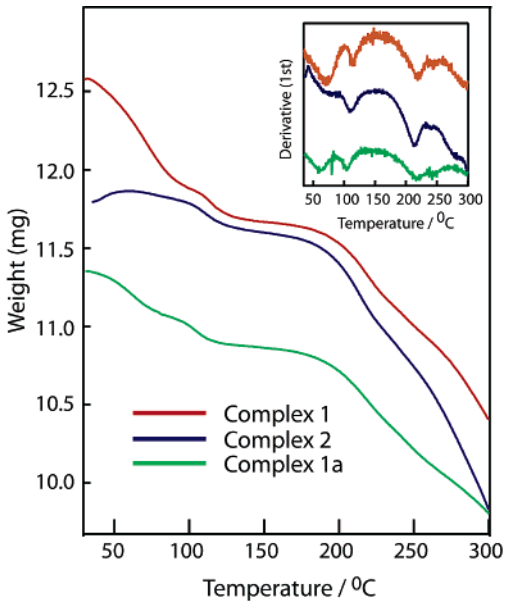

Figure 1. TGA plot of **1**, **2**, and **1a** with derivative (DTA) plot of TGA as inset.

Results and Discussion

Synthesis and Characterization. Upon mixing $Fe^{III}(NO_3)_3\cdot 9H_2O$, H_2S-L, NaOH, and NaOAc at 1:1:2:3 ratio in MeOH, the solution turned red-purple. Diffusion of diethyl ether at low temperature afforded complex **1** (**1a** with H_2R-L) as diamond shaped crystals in ∼60−65% yield. In the IR spectra of **1** and **1a**, the peaks at 1640 and 1365 cm^{-1} were identified as asymmetric and symmetric carboxylate stretches, respectively, originating from the coordinated ligand.[10] The two bands at 1544 and 1452 cm^{-1} were attributed to the ν_{asym} and ν_{sym} stretching modes of the acetate anion coordinated to the Fe^{III} centers in the bridging form.[10] Both the complexes also show broad stretches at 3410 cm^{-1} and two sharp stretches at 3185, 3111 cm^{-1} due to OH (water or H-bonded OH) stretch and N−H stretches (from ligand), respectively. The elemental analysis supports the formulation of the complexes as $[Fe_2(OAc)(OH)(S\text{-L})_2]\cdot 4H_2O$ (**1**), $[Fe_2(OAc)(OH)(R\text{-Salhis})_2]\cdot 2H_2O$ (**1a**), and $[Fe_2(OAc)(OH)(S\text{-L})_2]\cdot H_2O$ (**2**). The TGA between 30 and 95 °C shows weight loss corresponding to 2.5 mol of H_2O for **1**, 1 mol H_2O for **1a** and no loss for **2** (Figure 1). Weight loss between 95 and 140 °C corresponds to 1 mol of water for **1** and **2**. This accounts for the water content in the formulation closely as

(8) Blessing, R. *Acta Crystallogr., Sect. A* **1995**, *51*, 33.
(9) Sheldrick, G. M. *SHELXL-97*: *Program for Crystal Structures Refinement*; University of Göttingen: Göttingen, Germany, 1997.
(10) Nakamoto, K. *Infrared and Raman Spectra of Inorganic Compounds*, 5th ed.; Part B; Wiley-Interscience: New York, 1997. Carboxylate and acetate stretchings were distinguished by comparing the ligand IR as well as that of the copper complex reported earlier, ref 7.

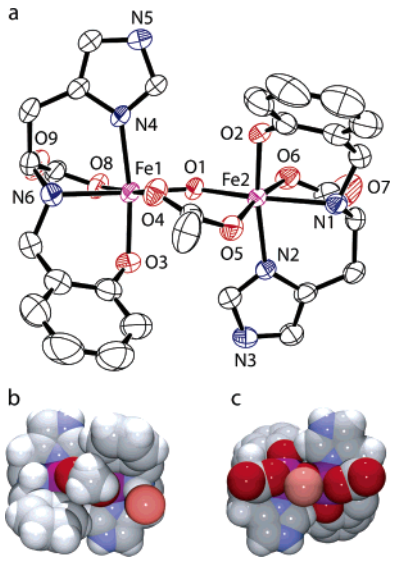

Figure 2. (a) Molecular structure of **1** with thermal ellipsoids set to 50% probability level. (b) Space filling model showing cavity around bridging acetate and (c) hydrophilic cavity around hydroxide bridge.

well as shows that two types of water bonding are present in the crystals of **1** and **2** (see structural discussion). The molar conductance of **1** and **1a** in MeOH were found to be 12 and 20 S cm^2 mol^{-1}, respectively, supporting the nonionic formulation (expected for 1:1 electrolyte in methanol 85−115 S cm^2 mol^{-1}).[11] However, as the protons of the bridged hydroxide are usually acidic, partial ionization in polar solvent might be the reason for low conductance observed. The room temperature magnetic moments of **1** and **1a** are 4.57 and 4.38 μ_B/iron, respectively. The susceptibility data obtained for **1** and **2** between 18 and 305 K fit well with a binuclear high-spin Fe(III) model yielding J values of −14.3 and −15.3 cm^{-1}, respectively (Supporting Information), and commensurate with values observed for other weak antiferromagnetically coupled hydroxo-bridged binuclear iron(III) complexes.[12]

Crystal Structures of 1 and 1a. Complex **1** crystallized in the chiral space group $P6_1$ (No. 169) and **1a** in the opposite chiral space group $P6_5$ (No. 170). Structures of **1** and **1a** are mirror images of each other. Thus discussions below for **1** are applicable to **1a** as well. The molecular structure of **1** with atom numbering scheme is shown in Figure 2.

In **1**, each of the two hexadentate irons is ligated with a tetradentate [*S*-$(L)^{2-}$] and is bridged through one hydroxo and one bidentate acetate ligand. The Fe−O1 distances (∼1.97 Å, Table 2) are characteristic of the Fe(III)−OH bridge and are significantly higher than those of Fe(III)−oxo bridge distances (<1.8 Å).[12,13] Hydroxo-bridged diiron(III) complexes are fewer compared to oxo-bridged complexes.[12,13a,14] The presence of two triply charged iron(III)

Table 2. Selected Bond Lengths (Å) and Angles (deg) of the Complexes

	1	**1a**	**2**
Fe1···Fe2	3.5175(7)	3.522	3.522
Fe1−O1	1.9722(18)	1.971(2)	1.969(3)
Fe1−O4	1.9875(26)	1.997(2)	1.995(3)
Fe1−N4	2.1314(23)	2.136(3)	2.142(4)
Fe1−N6	2.2030(22)	2.220(3)	2.211(4)
Fe1−O3	1.9463(19)	1.961(2)	1.957(3)
Fe1−O8	1.9988(26)	2.001(2)	2.000(3)
Fe2−O1	1.9695(21)	1.968(2)	1.972(3)
Fe2−O5	2.0309(24)	2.034(2)	2.031(3)
Fe2− N2	2.1400(22)	2.141(3)	2.151(4)
Fe2−N1	2.2006(22)	2.211(3)	2.206(3)
Fe2−O2	1.9314(19)	1.943(2)	1.94693)
Fe2−O6	2.0179(24)	2.024(2)	2.016(3)
Fe1−O1−Fe2	126.35(11)	126.83(12)	126.69(16)
N4−Fe1−O3	169.24(0.09)	168.88(11)	169.22(15)
O4−Fe1−N6	93.99(0.09)	94.17(11)	94.13(14)
N6−Fe1−O8	77.90(0.10)	78.01(11)	77.51(14)
O8−Fe1−O1	94.37(0.09)	94.10(10)	94.60(13)
O1−Fe1−O4	93.62(0.09)	93.59(10)	93.69(12)
N2−Fe2−O2	168.62(0.09)	168.36(11)	168.76(13)
O5−Fe2−N1	97.14(0.08)	97.56(9)	97.08(12)
N1−Fe2−O6	76.49(8)	76.07(10)	76.45(12)
O6−Fe2−O1	90.56(0.09)	90.53(10)	90.84(13)
O1−Fe2−O5	95.63(0.09)	95.66(9)	95.43(12)

species usually makes the hydroxide proton acidic, leading to the formation of an oxo-bridged complex.[13a] An [Fe^{III}(μ-OH)(μ-carboxylato)Fe^{III}]$^{4+}$ core has been proposed in the active site of protein mammalian purple acid phosphatase.[15] Complexes with [Fe^{III}(μ-OH)(μ-carboxylato)$_2Fe^{III}$]$^{3+}$ [12b] and [Fe^{III}(μ-O)(μ-carboxylato)Fe^{III}]$^{3+}$ [13b] cores have been characterized before, but **1** with the [Fe^{III}(μ-OH)(μ-carboxylato)-Fe^{III}]$^{4+}$ core resembles the active site of protein mammalian purple acid phosphatase more closely. Further, the imidazole, phenolate, and carboxylate donors in the ligand resemble the histidine, tyrosine, and aspartate donor present in the protein.

The conformation at the chiral carbon of the ligand is *S* in **1** and *R* in **1a**. In addition to the asymmetric carbon center in the ligand, the coordination of amine N to the iron gives rise to an asymmetric secondary nitrogen atom, N1 and N6, which has the *R* configuration in **1** and *S* configuration in **1a**. This phenomenon of opposite conformation preference at chiral carbon and amine N has been observed in all the characterized complexes of this ligand.[7,16] This is important because this eliminates the formation of a diastereoisomer (C and N having same conformation). The lower dihedral angles between Fe−N amine and the methylene arm of the phenolate rings result in a folding of the phenolate ring forming a bowl shaped C_2 symmetric chiral and essentially hydrophobic cavity around the bridging acetate (Figure 2b).

For complex **1**, the lattice diagram viewed normal to the 001 plane shows hexagonal channels filled with water from one end to the other end of the crystals (Figure 3). The molecules of **1** with hydroxo bridge facing the channel have a water molecule within H-bonding distance of the hydroxo

(11) Geary, W. J. *Coord. Chem. Rev.* **1971**, *7*, 81.
(12) (a) Thich, J. A.; Ou, C. C.; Powers, D.; Vasiliou, B.; Mastropaolo, D.; Potenza, J. A.; Schugar, H. J. *J. Am. Chem. Soc.* **1976**, *98*, 1425. (b) Turowski, P. N.; Armstrong, W. H.; Liu, S.; Liu, S.; Brown, S. N.; Lippard, S. J. *Inorg. Chem.* **1994**, *33*, 636.
(13) (a) Armstrong, W. H.; Lippard, S. J. *J. Am. Chem. Soc.* **1984**, *106*, 4632. (b) Yan, S.; Que, L., Jr.; Taylor, L. F.; Anderson, O. P. *J. Am. Chem. Soc.* **1988**, *110*, 5222.
(14) (a) Murch, B. P.; Bradley, F. C.; Boyle, P. D.; Papaefthymiou, V.; Que, L., Jr. *J. Am. Chem. Soc.* **1987**, *109*, 7993. (b) Borer, L.; Thalken, L.; Ceccarelli, C.; Glick, M.; Zhang, J. H.; Reiff, W. M. *Inorg. Chem.* **1983**, *22*, 1719.
(15) Lindqvist, Y.; Johansson, E.; Kaija, H.; Vihko, P.; Schneider, G. *J. Mol. Biol.* **1999**, *291*, 135.
(16) Voss, K. E.; Angelici, R. J.; Jacobson, R. A. *Inorg. Chem.* **1978**, *17*, 1922.

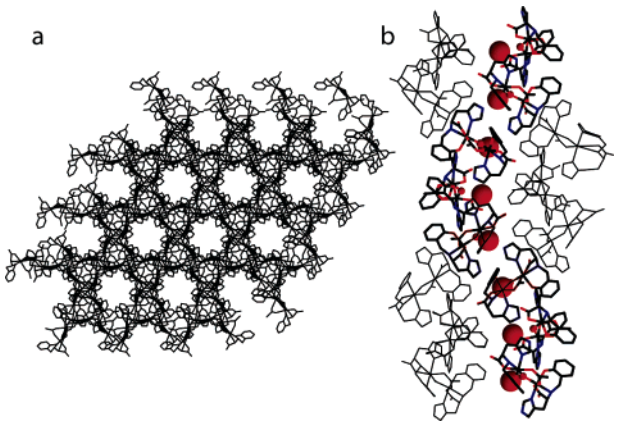

Figure 3. (a) Channels in **1** through 001 plane. (b) Side view of one channel showing the water (red) H-bonded to OH bridge of **1**.

bridge (O1−O11 2.6961 Å). The crystals of **1a** have identical but left-handed helices.

A notable feature of the molecule is the formation of a crescent moon shaped hydrophilic binding site (Figure 2c) formed by lining up the hydroxo bridge (H-bond donor) and all four oxygen atoms of the carboxylate oxygen (H-bond acceptor). The helical channels were formed by docking of dimers on top of each other rotated by 60° and connected through intermolecular hydrogen bonding between imidazole proton and phenolate oxygen (Figure 4a).[17] Other H-bonding interactions present in the lattice are shown in Figure 4b,c. As the bridging hydroxo proton in a diiron(III) center is acidic,[12b,13a] the molecules of **1** form a channel with helical hydrophilic cavities with an acidic proton (Figure 5). The helical array of acidic proton together with a hydrophilic cavity inside the channel has the potential to influence binding and reaction inside the channel and is a feature which distinguishes **1** from previously characterized channels.[2,5,6] The neighboring molecules of **1** in the channel (Figure 3b, thin lines) have a methyl group of acetate and an aromatic ring facing the hydrophilic cavity. Thus, except for hydrophilic cavities, the rest of the inner surface of the channel is hydrophobic. The channel diameter calculated using atom to atom distances from bridging oxygen (O1) to facing phenolate carbon (C11) is 7.35 Å and the methyl carbon of acetate bridge (C24) to facing carboxylate oxygen (O8) is 9.81 Å (Supporting Information). This is intermediate between the other two reported helical channels (∼11 Å[4a] and 5.5 Å[4b]).

Out of the four molecules of water present in **1**, one (O13a) is within the hydrogen bonded distance of a bridging hydroxo group (O1···O13a 2.77 Å) and another (O10) forms a hydrogen bonded bridge between carboxylate and neighboring amine (Figure 4c).[17] Two waters in similar positions were also present in **1a**. Three waters including one H-bonded to bridging hydroxide (O13a) in the channels of **1** are disordered over several positions and have refined with shared occupancy (Supporting Information). However, in **1a**, only one water is present inside the channel H-bonded to bridging hydroxide with full occupancy. Thus, two different types of H-bonded waters have been observed: (a) water inside the channel and (b) one forming bridge (O10) between two neighboring **1** species (Figure 4c). As the waters inside the channel are loosely bound compared to the other water (O10), the waters inside the channel can be removed easily, and the quantity tends to vary from crystal to crystal (three disordered in **1**, two in **1a**). The loss of water in two different temperature ranges (<100 and 100−140 °C) observed in TGA agrees well with two types of water in the crystal. The loss of water at relatively low temperature (30 °C onward) has been observed for another coordination complex with channels.[4b]

Empty Channels in 2. Taking a cue from TGA, the crystals of **1** were heated at 95 °C under reduced pressure for 2 h and then structurally characterized (**2**). Structural parameters and bond parameters of **2** are mostly unchanged compared to **1** (Tables 1 and 2). As expected, waters from inside the channel are absent in **2**, but the water (O10) H-bonded between two molecules of **1** remains unchanged. TGA of **2** shows no or negligible weight loss between 30 and 95 °C and weight loss of 1.84% (corresponds to 0.8 mol of water per molecule) between 95 and 140 °C in

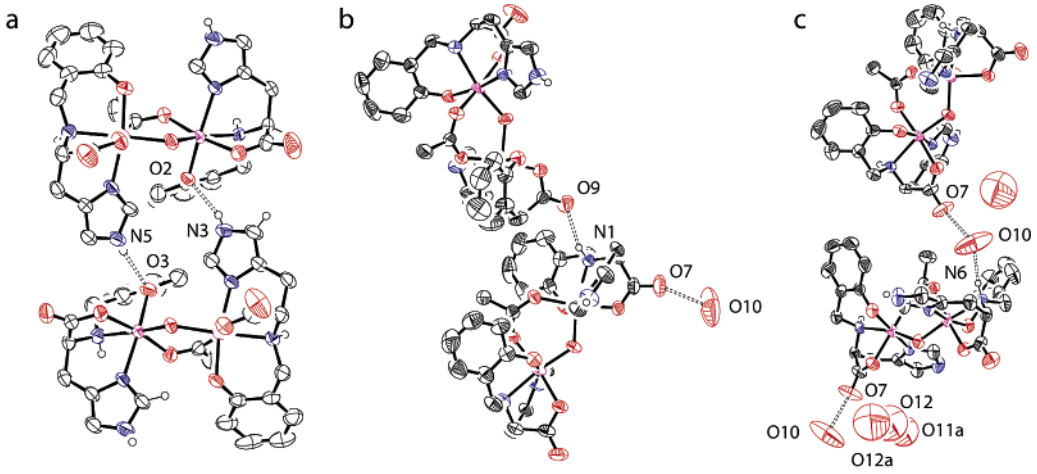

Figure 4. Intermolecular hydrogen bonding responsible for the (a) formation of the helix, and (b and c) stabilization of the lattice.

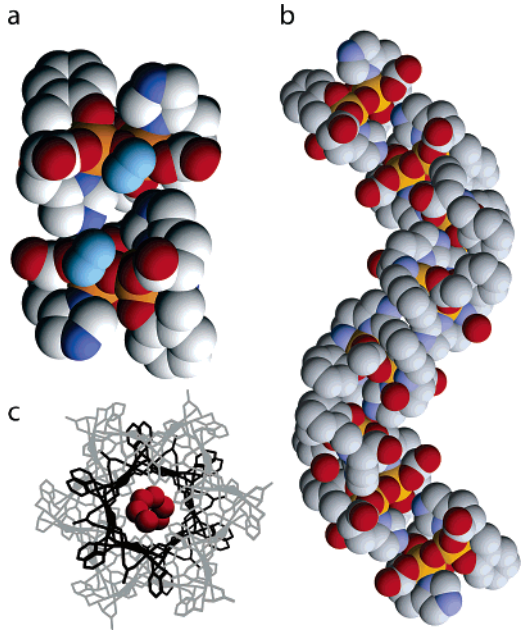

Figure 5. (a) Docking of one dimer on top of another through H-bonding interaction (b) forms a helix of hydrophilic cavity constituting (c) the helical channel in the crystal of **1**.

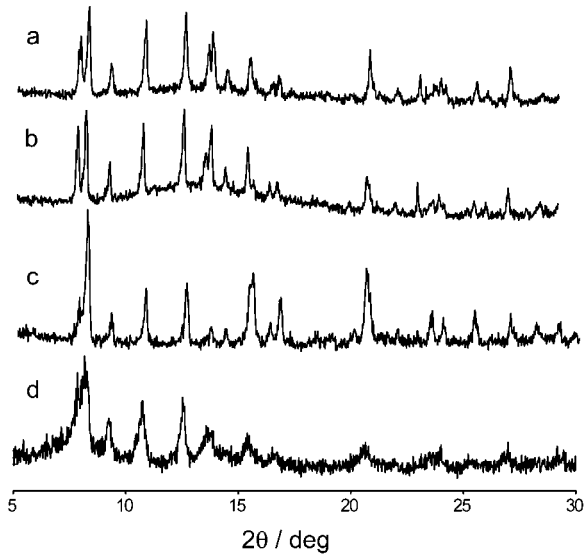

Figure 6. X-ray powder diffraction pattern of (a) **1**, (b) **2**, (c) **3**, and (d) **1** dried at 140 °C.

agreement with the structural observation. Sharp lines and patterns in X-ray powder diffraction (XRPD) of **1** and **2** also show that the crystals retain their identity also in the bulk (Figure 6). Thus, X-ray structural data, TGA, and powder diffraction together show that the solvents (water) can be selectively removed from the channels without destroying the channels, forming porous single crystals or powder with empty channels. This is in contrast with the other two reported helical channels, wherein one case removing the waters thermally from the channels destroys the H-bonded network yielding amorphous powder[4b] and in another case[4a] removal of water from the channel has not been tried.

After heating the crystals at 140 °C for 2 h under vacuum, crystals retain their shape but do not diffract well enough to get a structure. The TGA of this sample does not show any appreciable weight loss between 30 and 140 °C confirming the loss of all water of crystallization. The XRPD (Figure 6d) shows retention of some sharp lines but loss of fine lines. As the H-bonding network was formed mainly from intermolecular H-bonding between the ligands (Figure 4), the network remains stable even after removing waters from the channels. However, loss of the last water (O10) possibly destroys the network (at least partially). The choice of a ligand with both H-bond donor and acceptor in equal number (donor, amine; imidazole and acceptor, carboxylate, coordinated phenolate) might have helped to form a stable network.

Refilling the Channel with I_2. To check if small molecules can be inserted in the channel, similar to the Kitagawa group's[1d] report on one-dimensional array of oxygen molecules inside a microporous (4 × 6 Å) Cu(II) coordination polymer and the Lu group's[18] I_2 incorporation in 2D channels, we had exposed a few crystals of **1** to I_2 vapors in a closed container for 5−7 days. Structural analysis of these crystals has met with limited success. The resolution of the structure was poor,[19] and iodines have high thermal parameters. The structure could be solved with iodine inside the channel only. The high molecular weight iodines are unlikely to be mistaken with any other atom. The I−I distance matches with that of molecular iodine (2.6 Å). Surface adsorption which is likely to be random should not affect structural characterization. The higher thermal parameter of iodine (alternative explanation: disordered iodine between two slightly different orientation) in the structure might have resulted from the absence of any strong binding force for iodine inside the channel, thus allowing iodine some degree of freedom to move.

Iodination of the coarsely ground crystals (100−150 mg batches) was also performed for bulk measurement. On the basis of the iodine estimation[20] and elemental analysis, it was formulated as $[Fe_2(\mu\text{-OH})(\mu\text{-OAc})L_2]\cdot H_2O\cdot 0.6I_2$ (Experimental Section). Iodine estimations were also performed after thoroughly washing the iodine doped crystals with CCl_4 to remove traces of iodine from the surface. The iodine estimated was 13% (washed) as opposed to 17% (unwashed). Thus, while minor surface adsorption (4%) might have occurred, a significant amount of iodine is not easily removable. TGA of the crystals doped with iodine shows gradual weight loss of 17% up to 250 °C. The TGA sample after heating at 250 °C was analyzed and found to contain 4% iodine. Deducting the expected 7% weight loss for the corresponding empty crystals (**2**) in the same temperature range and adding the 4% iodine found after heating, the total

(17) Range for N−H···O distances 2.69−2.98 Å; O−H···O distance 2.74−3.004 Å. (a) Couchman, S. M.; Jeffery, J. C.; Ward, M. D. *Polyhedron* **1999**, *18*, 2633. (b) Pal, S.; Sankaran, N. B.; Samanta, A. *Angew. Chem., Int. Ed.* **2003**, *42*, 1741.

(18) Lu, J. Y.; Babb, A. M. *Chem. Commun.* **2003**, 1346.

(19) Crystallographic data for **3** follow: mounted on a glass capillary, $C_{28}H_{32}Fe_2I_2N_6O_{10}$, hexagonal space group, $P6_1$, $a = b = 13.2725(10)$ Å, $c = 36.032(6)$ Å; $\alpha = \beta = 90°$, $\gamma = 120°$; $V = 5497.0(11)$ Å^3, $Z = 6$, $\rho_{calcd} = 1.773$ Mg/m^3, R1 = 0.1072, wR2 = 0.2855 ($I > 2\sigma(I)$); R1 = 0.1434, wR2 = 0.3172 (all data), GOF on $F^2 = 1.188$. See Supporting Information.

(20) Benesi, H. A.; Hildebrand, J. H. *J. Am. Chem. Soc.* **1949**, *71*, 2703.

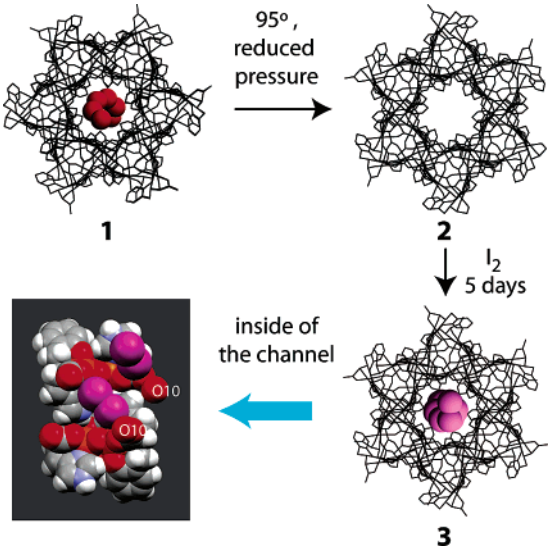

Figure 7. The removal of water and insertion of I_2 inside the channel.

amount of iodine (14%) from TGA studies is closer to the value obtained from titrimetric analysis (17%). Surface adsorbed iodine, a volatile solid, cannot be retained at 250 °C. These experiments suggest that the channels in the bulk sample can be partially filled with external dopant. The XRPD pattern of **3** (Figure 6c) shows enhancement, notably at 8.1°, 15.7°, 16.5° (corresponding to 2.6 Å, I−I distance) supporting partial filling of channels in the bulk sample with iodine. The overall process has been shown schematically in Figure 7.

Rehydration of the Channel. The crystals of **2** and similarly dried crystals of **1a** were exposed to water vapor in a closed container for 3 days followed by TGA to ascertain the amount of water absorbed. The TGA of **2** and dried **1a** after rehydration showed weight loss of 5.2% (∼2.5 water) and 4.3% (∼2 water) between 30 and 95 °C and weigh loss of ∼2.0% for both the samples between 95 and 140 °C (Supporting Information). This result supports that the channels can be refilled. This result also showed that the crystals of **1** and **1a** have slightly different water retention capacity despite being enantiomorphs to each other. Minor differences in the lattice parameter and bond parameter may have contributed to the difference in water uptake in the crystals. The channel diameter of **1**, calculated by atom to atom distances from bridging oxygen(O1) to facing phenolate carbon(C11), is slightly wider than in **1a** (7.35 Å for **1** compared to 7.30 Å for **1a**).

Conclusions. We were able to synthesize a microporous crystal with an empty 1D helical channel by selectively removing loosely bound waters. Evidence also points to successful insertion of iodine inside the channel (Figure 7). The distinguishing feature of these channels over others[4] is the helical arrangement of a hydrophilic cavity and acidic proton inside the channel (Figure 5). The strong charge-transfer transition and the enantiopurity of the crystals increase the potential as an optical material.

One interesting point observed in this set of complexes: the ligand has an effectively equal number of H-bond donors and acceptors (donor, amine, imidazole; acceptor, carboxylate, coordinated phenolate). This has reduced the dependence of network formation on external donor/acceptor, helping the lattice to be more thermally stable. Present work along with our earlier report[7] shows that enantiopure L^{2-} with its multipoint H-bonding capability (carboxylate, imidazole, amine, phenolate) can self-assemble differently with a different metal giving rise to symmetrically ordered materials as diverse as capsules to helices.

Acknowledgment. We thank Prof. A. R. Chakravarty and A. Mukherjee from IISc Bangalore, CDRI, Lucknow, India, Dr. A. Srinivasan, IIT Guwahati, and CSIR, New Delhi, for temperature dependent magnetic measurements, analytical data, XRPD measurements, and funding (Grant 01/(1669)/00/EMR-II to M.R. and 9/731(28)/2003-EMR-I to M.A.A.), respectively. Reviewer suggestions at the revision stage were very helpful.

Supporting Information Available: TGA plot of **1**−**3**, additional structural data and figures (PDF). Crystallographic data in CIF format. This material is available free of charge via the Internet at http://pubs.acs.org.

IC049145N